Density matrix and spin-dependent correlations of normal liquid ^{3}He

M. L. Ristig and K. E. Kürten
Institut für Theoretische Physik, Universität zu Köln, 5 Köln 41, Germany

J. W. Clark
McDonnell Center for Space Sciences and Department of Physics, Washington University, St. Louis, Missouri 63130
(Received 21 March 1978)

The influence of spin-dependent correlations on the one-body density matrix of a Fermi system is explored, for a normal-state wave function in which differing Jastrow factors are assigned to pairs in spin-projection states $\uparrow\uparrow$ and $\uparrow\downarrow$. The structural results of Ristig and Clark for state-independent Jastrow correlations are generalized by appealing to the commutativity of the assumed correlation operators and the topological properties of the diagrammatic representations of cluster expansions of the density matrix and corresponding occupation probability. Application to liquid ^{3}He (or the electron gas) calls for suitable spin-dependent spatial distribution functions. Such inputs may be supplied by Fermi hypernetted-chain theory adapted to σ_z-dependent correlations. The required extension is carried out for the Krotscheck-Ristig version of the theory, resulting in two coupled nonlinear integral equations for theoretical determination of the experimentally accessible spin-dependent radial distribution functions $g^{\uparrow\uparrow}(r)$ and $g^{\uparrow\downarrow}(r)$. Preliminary to a full implementation of this approach for liquid ^{3}He, the spin-dependent structure functions associated with a Jastrow factor of Schiff-Verlet type are determined.

I. INTRODUCTION

Substantial advances in the microscopic description of dense Fermi fluids have recently been recorded.[1,2] The ground-state energy per particle, the spatial distribution functions and static structure functions, and the momentum distribution and one-body density matrix have been evaluated in some detail for liquid ^{3}He and simple models of nuclear matter, based on variational ground-state wave functions of state-independent Jastrow type.[3-9] The development of methods for summing, to all orders, important classes of contributions to the cluster expansions of expectation values has played a pivotal role in these studies. Of special importance are the successful generalizations,[10-12] to Fermi statistics, of the hypernetted-chain (HNC) techniques long in use for the treatment of Bose and classical fluids.[13,14] It is equally significant that Monte Carlo algorithms are now available[5] for testing the accuracy of these new cluster summation procedures. Favorable comparisons of such procedures with Monte Carlo evaluations of the Jastrow energy and momentum distribution have been reported in Refs. 3 and 9, respectively.

It is now widely recognized that the simple Jastrow wave function,

$$\Psi = F\Phi, \quad F = \prod_{i<j}^{A} f(r_{ij}), \tag{1}$$

where Φ is the ground-state wave function of the noninteracting system, provides a valuable starting point for a true quantitative description of strongly interacting Fermi fluids. The next generation of studies is addressed to the incorporation of the essential state-dependent correlations absent from the Jastrow ansatz. In one general approach to this problem, the model function Φ is replaced by a complete set of energy eigenfunctions of the noninteracting system, and perturbative computations are performed in the correlated basis so generated.[13,15] In the second general approach (which may be combined with the first[16]), the correlation factor F itself is generalized to carry state dependence of varying degrees of complication.

Presently, the second approach is being energetically pursued toward a quantitatively accurate evaluation of the ground-state energy per particle of nuclear matter assuming realistic, highly state-dependent nucleon-nucleon interactions.[16-20] In this context it is necessary to assume a correlation operator F depending explicitly on tensor and spin-isospin operators.[17,21,22] Unfortunately these operators do not in general commute with one another. This complication presents a serious obstacle to acceptable generalization, to realistic nuclear matter, of the Fermi HNC procedures developed for wave function (1).

Here we shall focus instead on Fermi fluids like liquid ^{3}He and the electron gas, for which a useful and tractable generalization of the established Fermi HNC methods can be readily accomplished. These systems are of course quite important in their own right. Much effort has been directed toward a quantitative understanding of the ground-state correlations of the electron gas, which is one of the most fundamental models of

solid-state physics.[23,24] Normal liquid ^{3}He enjoys continued theoretical attention, while a new generation of experiments (and experimental facilities) is opening up the field of high-flux neutron scattering studies of this system.[25,26] Spin-dependent correlations, in particular, are beginning to play an interesting role. In principle, information on such correlations may be extracted from neutron- and x-ray scattering experiments.[27-30]

The interaction between two ^{3}He atoms (in the case of the electron gas, the Coulomb potential) does not depend significantly on the spin degrees of freedom. This property allows one to treat ^{3}He atoms with opposite spin as different particles; accordingly, the wave function need only be antisymmetric with respect to exchange of the coordinates of the constituents with the same spin projection.[31] A generalization of Eq. (1) appropriate to exploration of the effects of spin correlations (in addition to spatial correlations) is therefore provided by

$$\Psi = F^{\uparrow\uparrow} F^{\downarrow\downarrow} F^{\uparrow\downarrow} \Phi^{\uparrow\uparrow} \Phi^{\downarrow\downarrow}. \tag{2}$$

Ansatz (2) describes an antiferromagnetic two-component Fermi system, $\Phi^{\uparrow\uparrow}$ or $\Phi^{\downarrow\downarrow}$ being a Slater determinant of $A/2$ independent fermions of parallel spin. For the correlation operators we assume the conventional Jastrow form:

$$F^{\uparrow\uparrow} = \prod_{k<k'} f^p(r_{kk'}), \quad F^{\downarrow\downarrow} = \prod_{l<l'} f^p(r_{ll'}),$$
$$F^{\uparrow\downarrow} = \prod_{k<l} f^a(r_{kl}), \tag{3}$$

where k, k' (l, l') denote pairs of particles with spin up (spin down). By symmetry, the two-body correlation factors defining $F^{\uparrow\uparrow}$ and $F^{\downarrow\downarrow}$ must be identical. The independent correlation functions $f^p(r)$ and $f^a(r)$ approach unity for large distance r and are determined at small r to take care of the singular behavior of the potential.

For the explorations to come we replace ansatz (2) by the equivalent trial function

$$\Psi = F(1,\ldots,A)\Phi, \tag{4}$$

where Φ is again the ground-state wave function of A noninteracting fermions with spin projection $s = \pm 1$. The correlation operator $F(1,\ldots,A)$ is of the familiar pair-product form

$$F = \sum_{i<j} f(ij), \tag{5}$$

but the two-body factors are now spin-dependent operators,

$$f(12) = \tfrac{1}{2}[f^p(r) + f^a(r)] + \tfrac{1}{2}\sigma_{1z}\sigma_{2z}[f^p(r) - f^a(r)]. \tag{6}$$

Henceforth we shall abbreviate σ_{1z}, σ_{2z}, etc. as σ_1, σ_2, etc.

The state dependence (6) is particularly simple because all spin operators commute with one another. A study of the consequences of ansätze (4)–(6) may yield useful clues for dealing with the more robust forms of state dependence important in realistic nuclear matter.

This paper presents a detailed study of the one-particle density matrix associated with the trial state (2)–(3) or (4)–(6). We draw heavily from structural results derived earlier[6] for the density matrix based on ansatz (1)—results which we properly generalize. In addition, we extend one version of Fermi HNC theory[10,12] to deal with the spin-dependent correlations of (4)–(6). As a preliminary numerical application of our formalism, the spin-dependent structure functions are calculated assuming state-independent spatial correlations for which comparable Monte Carlo results are available.

The formal structure of the one-particle density matrix of a two-component Fermi fluid described by ansätze (2)–(3) or (4)–(6) is explored in Sec. II. In Sec. III we accomplish a partial summation analogous to the compact cluster summation of the function $Q(r)$ performed in Ref. 6. The generalization of the Fermi HNC procedure of Krotscheck and Ristig[10,12] is sketched in Sec. IV. This generalization is needed for a projected determination of optimal spin-dependent structure functions, which will serve as inputs in the evaluation of the one-particle density matrix of liquid ^{3}He. Section V collects some technical results which may help to elucidate the physical content of the structural results on the density matrix. Section VI is devoted to the aforementioned numerical evaluation of the spin-dependent structure functions of liquid ^{3}He for *spin-independent* correlations.

II. ONE-PARTICLE DENSITY MATRIX

The one-particle density matrix $\langle \vec{r}' | \Gamma_1 | \vec{r}'' \rangle$ corresponding to the ground state of a homogeneous isotropic Fermi fluid depends only on $r = |\vec{r}' - \vec{r}''|$. This quantity is related by a Fourier transformation

$$\langle \vec{r}' | \Gamma_1 | \vec{r}'' \rangle = n(r) = \frac{2}{(2\pi)^3} \int n(k) e^{i\vec{k}\cdot\vec{r}}\, d\vec{k}, \tag{7}$$

to the average occupation $n_{\hat{k}} = n(k)$ of single-particle orbital $\hat{k}$:

$$n_{\hat{k}} = \langle \Psi | a_{\hat{k}}^\dagger a_{\hat{k}} | \Psi \rangle / \langle \Psi | \Psi \rangle. \tag{8}$$

The operator $a_{\hat{k}}^\dagger (a_{\hat{k}})$ is the usual creation (destruction) operator for a fermion of momentum $\hbar k$ and specific spin projection, $s = \pm 1$. The one-particle

density matrix (7) is seen to coincide with the particle density $\rho = k_F^3/3\pi^2$ for vanishing distance r, where k_F is the Fermi wave number.

A powerful theory of the quantities (7) and (8) based on spatially correlated trial ground states of type (1) has been developed in Ref. 6 and applied numerically in Refs. 7–9. (For further formal developments, see Ref. 32.) The density matrix (7) is found to possess the structure

$$n(r) = \rho n[N_1(r) + N_2(r)]e^{-Q(r)}, \tag{9}$$

with the strength factor n given by $n = \exp Q(r=0)$. The deviation of the sum $N_1(r) + N_2(r)$ from unity reflects important exchange effects.

Furthermore, the occupation probability (8) may be decomposed as

$$n(k) = n[N(k) + N_1(k)], \tag{10}$$

in such a manner that the function $N_1(k)$ describes the effect of the Fermi medium. That is, $N_1(k)$ vanishes for $k > k_F$, and the discontinuity of the occupation probability at the Fermi surface is given by $nN_1(k = k_F)$.

The functions $Q(r)$, $N_1(r)$, $N_2(r)$, $N(k)$, and $N_1(k)$ are defined in terms of their cluster expansions, which contain only irreducible contributions.[6] Reference 6 presents also a compact cluster summation of the $Q(r)$ expansion, in terms of the successive spatial distribution functions $g_2(\vec{r}_1, \vec{r}_2) = g(r_{12})$, $g_3(\vec{r}_1, \vec{r}_2, \vec{r}_3), \ldots$ corresponding to the wave function (1). The contributions to the various cluster expansions may be represented most conveniently by generalized Ursell-Mayer graphs. The basics of this diagrammatic scheme for state-independent correlations of Jastrow type (1) may be found in Refs. 6 and 10.

To generalize the formalism and results of Ref. 6 to two-component Fermi fluids described by ansätze (2)–(3), we employ the equivalent expression (4) involving spin-dependent Jastrow correlations (5) and (6). It is essential to realize that result (9) rests on the topological structure of the cluster expansion for the probability (8) and the pair-product ansatz (1) with *commuting* factors $f(r_{ij})$. Consequently, the density matrix $n(r)$ and occupation probability $n(k)$ associated with the spin-dependent correlated state, Eq. (4)–(6), still exhibit the respective structural properties (9) and (10). The functions $Q(r)$, $N_1(r)$, $N_2(r)$, $N(k)$, and $N_1(k)$ are now of course functionals of $f^p(r)$ and $f^a(r)$, and are thus more complicated than for the ansatz (1), i.e., for $f^p(r) = f^a(r)$. Nevertheless, we may represent the cluster expansions which define these five quantities by the same sets of diagrams as given in Ref. 6, provided we adopt an appropriate generalization of the graphical rules.

A wavy line connecting two dots, labeled say 1 and 2, stands for the spin-dependent operator

$$\zeta(12) = f(12) - 1 = \zeta^m(r_{12}) + \zeta^s(r_{12})\sigma_1\sigma_2$$
$$= \zeta^p(r_{12})\tfrac{1}{2}(1 + \sigma_1\sigma_2) + \zeta^a(r_{12})\tfrac{1}{2}(1 - \sigma_1\sigma_2). \tag{11}$$

A dashed line depicts the operator

$$\eta(12) = f^2(12) - 1 = \eta^m(r_{12}) + \eta^s(r_{12})\sigma_1\sigma_2$$
$$= \eta^p(r_{12})\tfrac{1}{2}(1 + \sigma_1\sigma_2) + \eta^a(r_{12})\tfrac{1}{2}(1 - \sigma_1\sigma_2). \tag{12}$$

The superscript m indicates the overall (mass density) correlation

$$\zeta^m(r) = \tfrac{1}{2}[f^p(r) + f^a(r) - 2], \tag{13}$$

and the superscript s refers to the spin-density correlation

$$\zeta^s(r) = \tfrac{1}{2}[f^p(r) - f^a(r)]. \tag{14}$$

A light oriented line represents the exchange operator

$$l(12) = \tfrac{1}{2}(1 + \sigma_1\sigma_2)l(k_F r_{12}), \tag{15}$$

where $l(x)$ is the Slater exchange function $l(x) = 3x^{-3}(\sin x - x\cos x)$. Note that this convention differs from that introduced earlier.[6,8] Equation (15) expresses quite plainly the fact that Pauli exclusion applies only to fermions with parallel spin projections.

A heavy oriented line represents a plane-wave function $A^{-1}e^{i\vec{k}\cdot\vec{r}_{12}}$. A solid dot labeled 1 implies a factor ρ together with an integration $\int d\vec{r}_1$ and an average over the spin projection s_1 of the particle at point 1. Two open dots, labeled 1 and 2, imply if present a dependence of the corresponding contribution on the separation $r = |\vec{r}_1 - \vec{r}_2|$ and the spin operator $\sigma_1\sigma_2$. Similarly, three open dots, labeled 1, 2, and 3, imply a dependence on the spatial coordinates $\vec{r}_1$, $\vec{r}_2$, $\vec{r}_3$ and the spin operators $\sigma_1\sigma_2$, $\sigma_1\sigma_3$, $\sigma_2\sigma_3$. The oriented lines will always form closed loops, if two open dots joined by them are counted as one.

In contrast to the rules of Refs. 6, 8, 10, no statistical weight factor need be assigned to any loop. Its effect is already absorbed in the spin-dependent form (15) of the exchange operator $l(12)$.

In order to make the graphical formalism more accessible, we have collected in the appendix a number of typical cluster expressions and their diagrammatic counterparts.

Equipped with the above generalized graphical rules we may represent the cluster series

$$N(k) = [\Delta N(k)]_2 + [\Delta N(k)]_3 + \cdots \tag{16}$$

and

$$N_1(k) = [\Delta N_1(k)]_1 + [\Delta N_1(k)]_2 + [\Delta N_1(k)]_3 + \cdots \tag{17}$$

which define the functions $N(k)$ and $N_1(k)$ associated with the states (4)–(6), by the sets of graphs given,

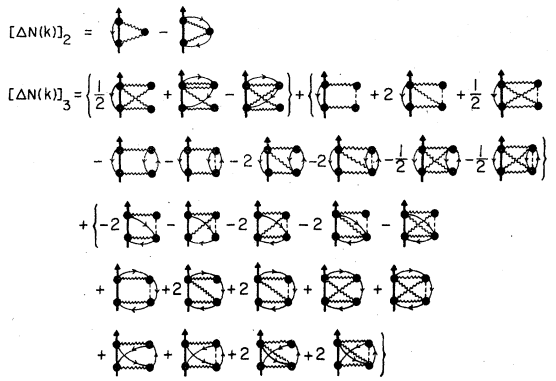

FIG. 1. Graphical representation of the two- and three-body contributions to the cluster expansion defining $N(k)$.

respectively, in Figs. 2 and 4 of Ref. 6. Figure 1 shows the two- and three-body cluster contributions to the function $N(k)$, while Fig. 2 depicts the two- and three-body portions of $N_1(k)$. The step function $[\Delta N_1(k)]_1 = \Theta(k_F - k)$ originates from the statistical properties of the noninteracting Fermi gas.

Similarly, the strength factor n appearing in Eq. (10) is given by[6]

$$\ln n = Q(r=0) = 2D[\zeta] - D[\eta]. \tag{18}$$

The functional $D[\zeta]$ is defined by the cluster expansion

$$D[\zeta] = (\Delta D[\zeta])_2 + (\Delta D[\zeta])_3 + (\Delta D[\zeta])_4 + \cdots . \tag{19}$$

Its diagrammatic representation is indicated in Fig. 3.

We next turn to the ingredients $N_1(r)$, $N_2(r)$, and $Q(r)$, which form via (9) the one-particle density matrix of the correlated states (4)–(6). It is most convenient to introduce, in analogy to the scheme of Refs. 6, 9, the (spin-dependent) operators

$$N_1(12) = [\Delta N_1(12)]_1 + [\Delta N_1(12)]_2 + [\Delta N_1(12)]_3 + \cdots , \tag{20}$$

$$N_2(12) = [\Delta N_2(12)]_2 + [\Delta N_2(12)]_3 + \cdots , \tag{21}$$

$$Q(12) = [\Delta Q(12)]_2 + [\Delta Q(12)]_3 + \cdots . \tag{22}$$

The leading cluster contributions are represented by the diagrams shown in Figs. 4, 5, and 6 (or in Figs. 7, 9, and 8 of Ref. 6). We stress that the more general interpretation adopted here, in which dynamical lines stand for commuting operators, allows the treatment of more complex systems than is possible with the version of the theory explored in Ref. 6.

The constituents $N_1(r)$, $N_2(r)$, and $Q(r)$ of structural result (9) follow as spin averages:

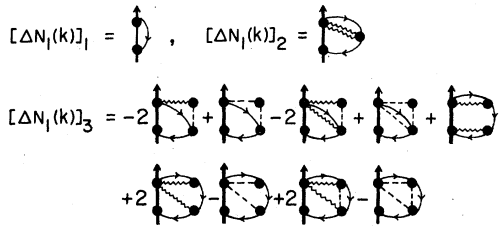

FIG. 2. Graphical representation of the two- and three-body contributions to the cluster expansion defining $N_1(k)$. The first diagram depicts the occupation probability for noninteracting fermions.

$$N_1(r) = \frac{1}{2}\sum_{s_1 s_2} \langle s_1 s_2 | N_1(12) | s_1 s_2 \rangle,$$

$$N_2(r) = \frac{1}{2}\sum_{s_1 s_2} \langle s_1 s_2 | N_2(12) | s_1 s_2 \rangle,$$

$$Q(r) = \frac{1}{2}\sum_{s_1 s_2} \langle s_1 s_2 | \tfrac{1}{2}(1+\sigma_1\sigma_2) Q(12) | s_1 s_2 \rangle. \tag{23}$$

Equivalently, we may introduce the operator

$$n(12) = \rho n [N_1(12) + N_2(12)] e^{-Q(12)} \tag{24}$$

and derive the one-particle density matrix for a Fermi fluid described by the wave functions (2)–(3) or (4)–(6) as the trace of expression (24):

$$n(r) = \frac{1}{2}\sum_{s_1 s_2} \langle s_1 s_2 | n(12) | s_1 s_2 \rangle. \tag{25}$$

Relation (25) follows if we observe the properties:

$$N_1(12) = \tfrac{1}{2}(1+\sigma_1\sigma_2) N_1(r),$$

$$N_2(12) = \tfrac{1}{2}(1+\sigma_1\sigma_2) N_2(r). \tag{26}$$

III. COMPACT CLUSTER SUMMATION

In Ref. 6 massive partial resummations of the cluster expansion of the function $Q(r)$ were accom-

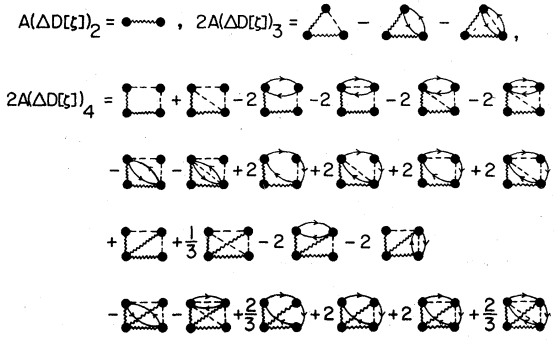

FIG. 3. Graphical representation of the two-, three-, and four-body contributions to the cluster expansion defining the functional $D[\zeta]$.

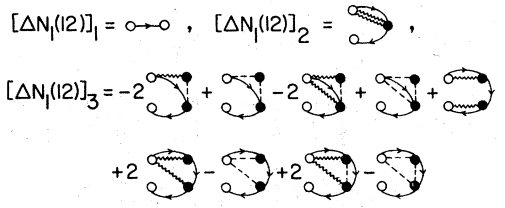

FIG. 4. Graphical representation of the exchange operator of noninteracting fermions and the two- and three-body contributions to the cluster expansion of the operator $N_1(12)$.

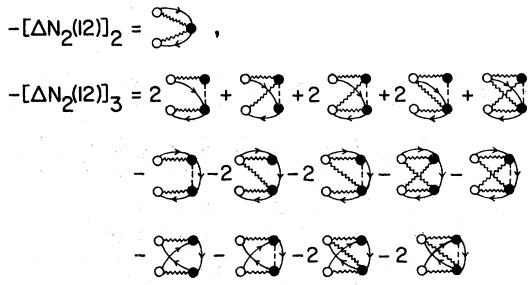

FIG. 5. Graphical representation of the two- and three-body contributions to the cluster expansion of the operator $N_2(12)$.

plished in terms of spatial distribution functions corresponding to the Jastrow wave function (1). This procedure may be applied as well to the cluster expansion (22) of the operator $Q(12)$ associated with the more general wave functions (4)–(6). We arrive at

$$Q(12)=[\Delta Q(12)]^{[1]}+[\Delta Q(12)]^{[2]}+\cdots . \tag{27}$$

For use in relation (18) we obtain

$$D[\zeta]=(\Delta D[\zeta])^{[1]}+(\Delta D[\zeta])^{[2]}+(\Delta D[\zeta])^{[3]}+\cdots . \tag{28}$$

All terms appearing explicitly in Eqs. (27) and (28) are displayed graphically in Fig. 7.

The blob with two dots on it symbolizes the compact part, $g(12)-1$, of a spin-dependent distribution operator $g(12)$, which is defined by means of its cluster expansion

$$g(12)=[\Delta g(12)]_2+[\Delta g(12)]_3+\cdots . \tag{29}$$

The two- and three-body portions of $g(12)$ are represented diagrammatically in Fig. 8. In like fashion, the blob with three dots on it stands for $g(123)-g(12)-g(13)-g(23)+2$, where $g(123)$ is a three-body distribution operator, the lowest-order cluster approximation to which is explicated in Fig. 9. The graphical rules stated in Sec. II apply in the presence of these new elements; for example, the next-to-last diagram of Fig. 7 represents

$$2A(\Delta D[\zeta])^{[2]}=\sum_{ijk}\langle ijk|\zeta(12)\zeta(13)[g(23)-1]|ijk\rangle$$
$$=\frac{1}{8}\rho^3\sum_{s_1s_2s_3}\int d\vec{r}_1\,d\vec{r}_2\,d\vec{r}_3\,\langle s_1s_2s_3|\zeta(12)\zeta(13)[g(23)-1]|s_1s_2s_3\rangle. \tag{30}$$

Inspection of cluster expansion (29) reveals that the operator $g(12)$ is of the form

$$g(12)=g(r_{12})+\sigma_1\sigma_2 g^{\sigma}(r_{12}). \tag{31}$$

The "overall" component $g(r)$ may be identified with the radial distribution function[13]

$$g(r)=\tfrac{1}{2}[g^{\uparrow\uparrow}(r)+g^{\uparrow\downarrow}(r)], \tag{32}$$

while the coefficient of the spin operator $\sigma_1\sigma_2$ is the spin distribution function defined by

$$g^{\sigma}(r)=\tfrac{1}{2}[g^{\uparrow\uparrow}(r)-g^{\uparrow\downarrow}(r)]. \tag{33}$$

Here $g^{\uparrow\uparrow}(r)$ and $g^{\uparrow\downarrow}(r)$ are the radial distribution functions for particles with parallel and opposite spin directions, respectively.

The Fourier transforms of $g(r)-1$ and $g^{\sigma}(r)$ may be given direct physical interpretation in terms of (mass-) density and spin-density fluctuations. They define the liquid structure function $S(k)$ and the spin structure function $S^{\sigma}(k)$ through

$$S(k)=1+\rho\int[g(r)-1]e^{i\vec{k}\cdot\vec{r}}d\vec{r}$$
$$=\frac{1}{A}\frac{\langle\Psi|\rho_{\vec{k}}\rho_{-\vec{k}}|\Psi\rangle}{\langle\Psi|\Psi\rangle}, \tag{34}$$
$$S^{\sigma}(k)=1+\rho\int g^{\sigma}(r)e^{i\vec{k}\cdot\vec{r}}d\vec{r}=\frac{1}{A}\frac{\langle\Psi|\rho^{\sigma}_{\vec{k}}\rho^{\sigma}_{-\vec{k}}|\Psi\rangle}{\langle\Psi|\Psi\rangle}.$$

The operator $\rho_{\vec{k}}=\sum_1^A e^{i\vec{k}\cdot\vec{r}_j}$ produces the (mass-)

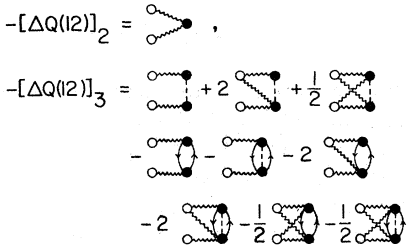

FIG. 6. Graphical representation of the two- and three-body contributions to the cluster expansion of the operator $Q(12)$.

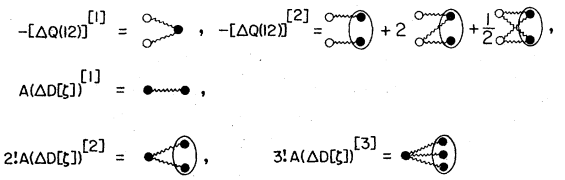

FIG. 7. Graphical representation of addends in the compact expansions of the operator $Q(12)$ and the functional $D[\zeta]$ in terms of the distribution operators.

density fluctuations; analogously, $\rho^{\sigma}_{\vec{k}} = \sum_1^A \sigma_j e^{i\vec{k}\cdot\vec{r}_j}$ generates the spin-density fluctuations. Quantities (34) may, in principle, be measured for liquid ^{3}He by means of neutron- and x-ray scattering.[23,24,27-30]

The three-body distribution operator $g(123)$ which appears in the term $(\Delta D[\zeta])^{[3]}$ has the structure

$$g(123) = g(\vec{r}_1, \vec{r}_2, \vec{r}_3) + [g^{\sigma}(\vec{r}_1, \vec{r}_2; \vec{r}_3)\sigma_1\sigma_2 + \text{c.p.}]. \quad (35)$$

Inspection of Fig. 9 demonstrates that the spin-independent component of (35) is the familiar (spin-averaged) three-body spatial distribution function,

$$g(\vec{r}_1, \vec{r}_2, \vec{r}_3) = \tfrac{1}{4}(g^{\uparrow\uparrow\uparrow} + g^{\uparrow\uparrow\downarrow} + g^{\uparrow\downarrow\uparrow} + g^{\downarrow\uparrow\uparrow}). \quad (36)$$

For the coefficient $g^{\sigma}(\vec{r}_1, \vec{r}_2; \vec{r}_3)$ one finds

$$g^{\sigma}(\vec{r}_1, \vec{r}_2; \vec{r}_3) = \tfrac{1}{4}(g^{\uparrow\uparrow\uparrow} + g^{\uparrow\uparrow\downarrow} - g^{\uparrow\downarrow\uparrow} - g^{\downarrow\uparrow\uparrow}). \quad (37)$$

The functions $g^{s_1 s_2 s_3} = g^{s_1 s_2 s_3}(\vec{r}_1, \vec{r}_2, \vec{r}_3)$ are the various three-body spatial distribution functions for fermions of specified spin projections. The connection of $g(\vec{r}_1, \vec{r}_2, \vec{r}_3)$ and $g^{\sigma}(\vec{r}_1, \vec{r}_2; \vec{r}_3)$ to density and spin-density fluctuations is made by transforming (36) and (37) into $\vec{k}$ space; we generate, respectively, the three-particle structure function[6,13]

$$S(\vec{k}_1, \vec{k}_2, -\vec{k}_1 - \vec{k}_2) = \frac{1}{A} \frac{\langle \Psi | \rho_{\vec{k}_1} \rho_{\vec{k}_2} \rho_{-\vec{k}_1 - \vec{k}_2} | \Psi \rangle}{\langle \Psi | \Psi \rangle} \quad (38)$$

and the quantity

$$S^{\sigma}(\vec{k}_1, \vec{k}_2, -\vec{k}_1 - \vec{k}_2) = \frac{1}{A} \frac{\langle \Psi | \rho^{\sigma}_{\vec{k}_1} \rho^{\sigma}_{\vec{k}_2} \rho_{-\vec{k}_1 - \vec{k}_2} | \Psi \rangle}{\langle \Psi | \Psi \rangle}. \quad (39)$$

The operators $N_1(12)$ and $N_2(12)$ are defined by their cluster expansions (20) and (21), respectively. It would be desirable to perform compact cluster summations for both quantities in analogy to the procedure executed for the operator $Q(12)$, as this would allow a more consistent numerical evaluation of $n(r)$ and $N(k)$ than has been achieved so far.[7-9] Such a treatment of $N_1(r)$ and $N_2(r)$ will become imperative once optimal correlation functions $f^p(r)$ and $f^q(r)$ become available, since the optimal functions are necessarily of long range, having components decaying only as r^{-2} for $r \to \infty$ (or as r^{-1} in the case of the electron gas). Optimal correlation functions could be determined in principle—and hopefully in practice—as solutions of Euler-Lagrange equations[33] based on Fermi HNC or other integral relations between the correlation and distribution functions.

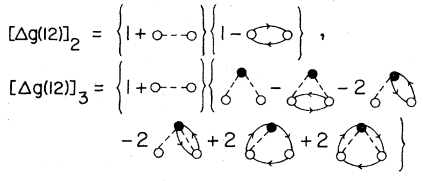

FIG. 8. Graphical representation of the two- and three-body contributions to the cluster expansion of the operator $g(12)$.

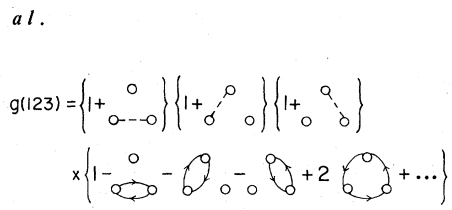

FIG. 9. Graphical representation of the cluster expansion of the operator $g(123)$.

For the state-independent Jastrow wave function of (1), Fantoni[32] has recently been able formally to sum the series for $Q(0)$ and $N(k) + N_1(k)$ in terms of series of basic[11,14] diagrams, by means of a complicated set of coupled nonlinear integral equations. It is of considerable interest to apply this formalism numerically to the helium liquids and to extend it to the σ_z-dependent correlations studied here. Work along these lines is in progress.

IV. TWO-COMPONENT FERMI HNC RELATION

As a first step toward determination of an essentially optimal correlation operator $f(12)$, one may develop generalized HNC relations that are suited to the spin-dependent correlations (6). In the next step one could establish Euler-Lagrange equations for $f(12)$ by proceeding along the lines of Lantto and Siemens' generalization[33] of the paired-phonon analysis[13,34] to Fermi fluids, that is, by functional variation of the energy expectation value with respect to $f^p(r)$ and $f^q(r)$ and an appropriate set of auxiliary functions, subject to the Fermi HNC relations as constraint.

Let us begin with the Fermi HNC scheme proposed by Krotscheck and Ristig[10,12] for state-independent correlations. Their formulation allows proper care to be taken, at each stage of approximation, of certain important effects of the exclusion principle. The relationships of the Krotscheck-Ristig version of Fermi HNC theory to that of Fantoni and Rosati[11] have been elucidated in Refs. 1 and 35.

The principal features of the Krotscheck-Ristig

approach are made explicit in terms of five characteristic functions, viz. $L(r)$, $P(r)$, $B(r)$, $\mathfrak{N}(r)$, and $R(r)$—or, equivalently, their conveniently normalized Fourier transforms $L(k)=\rho\int L(r)e^{i\vec{k}\cdot\vec{r}}\,d\vec{r}$, etc. The quantities $L(r)-\rho^{-1}\delta(r)$ and $P(r)$ are represented diagrammatically by the sums of all *non-nodal* diagrams[14] with two open dots having exchange lines attached to *both* of these points and to a chosen *one* of them, respectively. The quantity $B(r)$ is represented by the sum of all *elementary* diagrams[14] having *no* exchange lines attached to the two open dots present. The function $R(r)$ is a "dressed" or "renormalized" version of the correlation bond $\eta(r)=f^2(r)-1$; in Refs. 10 and 12 it was denoted by $\eta_R(r)$ or by $g_{DD}(r)$. The quantity $\mathfrak{N}(r)$, represented by the sum of all nodal diagrams[14] with two open dots and no exchange lines joining them, may be regarded merely as a redundant function which permits a convenient presentation of the HNC equation. This relation reads, for state-independent correlation functions $f(r)\equiv f^p(r)=f^a(r)$,

$$\mathfrak{N}(k)[1+R(k)L(k)]=R(k)\{1+R(k)L(k)-[1-P(k)]^2\} \quad (40)$$

together with

$$R(r)=f^2(r)\exp[\mathfrak{N}(r)+B(r)]-1. \quad (41)$$

Given suitable approximate inputs for the functions $L(k)$, $P(k)$, and $B(k)$, Eqs. (40)–(41) generate a corresponding approximant for the quantity $R(r)$. The functions $L(r)$, $P(r)$, and $B(r)$ can in turn be expressed more compactly in terms of the renormalized bond $R(r)$. Numerical calculations[4,36] for liquid ^{3}He indicate that simple approximations to L, P, and B of low order in the number of renormalized bonds may suffice. A reasonable starting point is provided by setting $L(k)=S_F(k)$ and $P(k)=B(k)=0$, where $S_F(k)$ is the static structure function of the noninteracting Fermi gas.[13] Such computational matters will be considered further in Sec. VI.

A connection of the dressed dynamical bond $R(r)$ with the liquid structure function—which is here the function of prime interest—may be established by the structural relation[12]

$$S(k)[1-P(k)]^2=L(k)[1+R(k)L(k)]. \quad (42)$$

We shall cast Eq. (42) into an abstract operator form suitable for generalization to the presence of spin-dependent correlations (6). First Eq. (42) is transformed into $\vec{r}$ space to obtain

$$G(r_{12})-2P(r_{12})+\rho\int P(r_{13})P(r_{23})\,d\vec{r}_3-2\rho\int P(r_{13})G(r_{23})\,d\vec{r}_3+\rho^2\int P(r_{13})G(r_{34})P(r_{24})\,d\vec{r}_3\,d\vec{r}_4$$
$$=\Delta L(r_{12})+R(r_{12})+2\rho\int R(r_{13})\Delta L(r_{23})\,d\vec{r}_3+\rho^2\int\Delta L(r_{13})R(r_{34})\Delta L(r_{24})\,d\vec{r}_3\,d\vec{r}_4 \quad (43)$$

with $G(r)=g(r)-1$ and $\Delta L(r)=L(r)-\rho^{-1}\delta(r)$. Symbolically we may write

$$G-2P+P^2-2PG+PGP=\Delta L+R+2R(\Delta L)+(\Delta L)R(\Delta L), \quad (44)$$

upon agreeing to define the product of two operators, say P and R, by

$$PR=\frac{1}{2}\rho\sum_{s_3}\int d\vec{r}_3\langle s_3|P(r_{13})R(r_{23})|s_3\rangle. \quad (45)$$

In the same way, the Fermi HNC relation (40) may be expressed in operator form as

$$\mathfrak{N}+\mathfrak{N}R+R(\Delta L)\mathfrak{N}=R^2+R(\Delta L)R-PRP+2PR. \quad (46)$$

Equations (44), (46), and (41) are derived purely from the topological structure of the underlying diagrammatic representation. Thus they are valid also in the more general case of differing correlation functions for pairs with parallel and antiparallel spins, $f^p(r)\neq f^a(r)$. All we need to do is to replace the various functions of relative distance r appearing in Eqs. (41), (44), (45), and (46) by the corresponding spin-dependent operators, i.e., $f(r)$, $G(r)$, $R(r)$, $L(r)$, $P(r)$, $B(r)$, and $\mathfrak{N}(r)\to f(12)$, $G(12)$, ... The operator quantities are defined by precisely the same sets of diagrams as their counterparts of the simpler case $f^p(r)=f^a(r)$; of course the new graphical rules spelled out in Sec. II are now to be applied. In particular, Figs. 10 and 11 give the diagrammatic contributions of low order in the cluster expansions of the operators $L(12)$,

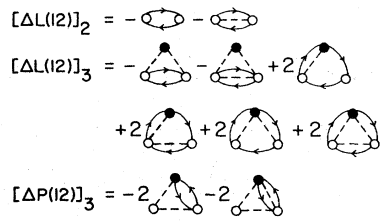

FIG. 10. Graphical representation of the two- and three-body contributions to the cluster expansions of the operators L and P.

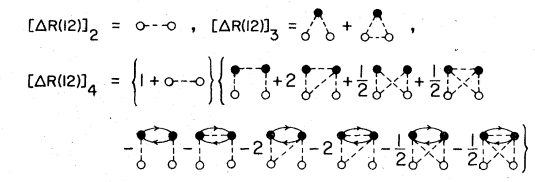

FIG. 11. Graphical representation of the two- three-, and four-body contributions to the cluster expansion of the dressed dynamical-bond operator $R(12)$.

$P(12)$, and $R(12)$,

$$\begin{aligned}\Delta L(12) &= [\Delta L(12)]_2 + [\Delta L(12)]_3 + \cdots \\ P(12) &= [\Delta P(12)]_3 + \cdots \\ R(12) &= [\Delta R(12)]_2 + [\Delta R(12)]_3 + [\Delta R(12)]_4 + \cdots .\end{aligned} \tag{47}$$

Further questions on representation, differing modes of classification of contributions, and partial summations are touched upon in Refs. 1, 4, 10, and 35.

Equation (46) together with the operator version of (41) amounts to two coupled nonlinear integral equations for the ingredients $R(r)$ and $R^\sigma(r)$ of the dressed dynamical-bond operator $R(12) = R(r) + R^\sigma(r)\sigma_1\sigma_2$. Upon specialization to $f^\flat = f^\alpha$, we have $R^\sigma(r) = 0$ and the original Fermi HNC equations (40) and (41) for state-independent correlations are recovered. Specialization to bosons, i.e., setting $\Delta L = P = 0$, yields the classical HNC scheme for a two-component Boltzmann system.[37]

We note that a generalization similar to the above has been carried through by Smith[38] in the framework of the Fantoni-Rosati approach to Fermi HNC theory.

V. REDUCTION TO $\vec{r}$ SPACE

Practical evaluation of the distribution functions $g^{\uparrow\uparrow}(r)$ and $g^{\uparrow\downarrow}(r)$ [or equivalently the structure functions $S(k)$ and $S^\sigma(k)$] via Eqs. (46) and (44), and the operator form of Eq. (41) begins with summation over the spin degrees of freedom. Thereby the operator HNC equations are recast as a set of two coupled integral equations.

Such reductions to $\vec{r}$ space are achieved by elementary algebraic manipulations which may be omitted here. However, additional physical insight can be gained by an examination of the pure $\vec{r}$-space versions of Eqs. (27), (20) and (21). To this end, we introduce further graphical elements. The function $\zeta^m(r)$ entering Eq. (11) is denoted by a wavy line bearing index m, while indices s, p, and a are attached to indicate the functions $\zeta^s(r)$, $\zeta^\flat(r)$, and $\zeta^a(r)$, respectively. Likewise, the functions $\eta^m(r), \ldots$ of Eq. (12) are represented graphically by dashed lines with indices $m, \ldots$. Further, a (light) oriented line with subscript p symbolizes the familiar exchange function $l(k_F r)$ of Eq. (15) (without the spin projector). A loop containing α points constructed from such exchange lines is accompanied by the weight factor $2^{\alpha-1}$ appearing in the original diagrammatic rules[6] for state-independent spatial correlations (1).

The $\vec{r}$-space versions of (20) and (21) are

$$\begin{aligned}N_1(r) &= [\Delta N_1(r)]_1 + [\Delta N_1(r)]_2 + \cdots , \\ N_2(r) &= [\Delta N_2(r)]_2 + \cdots .\end{aligned} \tag{48}$$

The cluster contributions appearing explicitly in (48) have the *same* diagrammatic representations as the corresponding terms of (20) and (21), except that a p index is to be associated with each line element. The higher contributions $[\Delta N_1(r)]_3$, $[\Delta N_2(r)]_3$, etc. involve sets of diagrams of rapidly growing complexity, with a line indices interspersed among the inevitable p labels.

The functional $D[\zeta]$ related to $Q(r=0)$ via Eq. (18) has the reduced graphical representation illustrated in Fig. 12. Consider the contribution $(\Delta D[\zeta])^{[2]}$. The two-dot blob labeled m represents the function $g(r) - 1$, and the blob with index s stands for the distribution function $g^\sigma(r)$. The term $(\Delta D[\zeta])^{[3]}$ involving the compact part of the three-body distribution operator $g(123)$ is decomposed into two qualitatively different portions. The first part contains a three-dot blob specified by index m, which represents the overall function $g(\vec{r}_1, \vec{r}_2, \vec{r}_3) - g(r_{12}) - g(r_{13}) - g(r_{23}) + 2$. The second part, describing the effect of the interference of mass- and spin-density fluctuations, involves the function $g^\sigma(\vec{r}_1, \vec{r}_2; \vec{r}_3) - g^\sigma(r_{12})$, which is depicted as a three-dot blob labeled ssm.

Elimination of the spin degrees of freedom generates a similar decomposition of the function $Q(r)$ into physically distinct portions. The first and second terms of its compact expression

$$Q(r) = [\Delta Q(r)]^{[1]} + [\Delta Q(r)]^{[2]} + \cdots \tag{49}$$

are displayed in Fig. 13. We notice that $Q(r)$ may be viewed as a superposition of three components; a first term (sum of diagrams with m labels only)

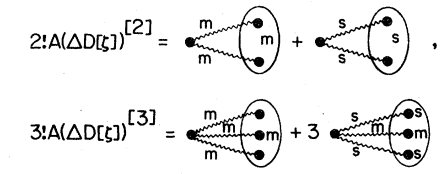

FIG. 12. Symbolic representation of the second and third addends of the compact expansion of $D[\zeta]$ in terms of mass- and spin-density distribution functions $g(r)$, $g^\sigma(r)$, $g(\vec{r}_1, \vec{r}_2, \vec{r}_3)$, $g^\sigma(\vec{r}_1, \vec{r}_2; \vec{r}_3)$.

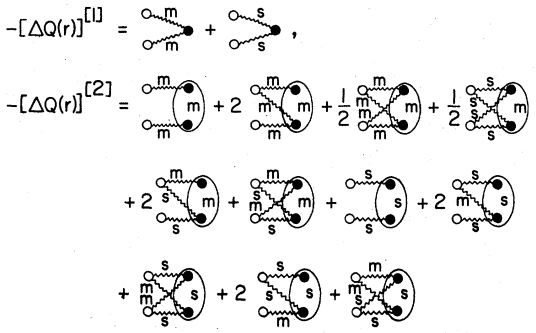

FIG. 13. Symbolic representation of the first two addends of the compact expansion of $Q(r)$ in terms of mass- and spin-density distribution functions.

which describes the effect of mass-density fluctuations, a second term (sum of diagrams with s labels only) arising from spin-density fluctuations, and a third term (diagrams with both s and m labels) which accounts for the interference of the two kinds of fluctuation. For completeness we provide in Fig. 14 the diagrammatic representation of the distribution functions involved, i.e., the functions $g(r)$ and $g^{\sigma}(r)$ or, more conveniently, $g^{\uparrow\uparrow}(r)$ and $g^{\uparrow\downarrow}(r)$.

VI. THEORETICAL STRUCTURE FUNCTIONS

To demonstrate the efficacy of essential components of the scheme described herein, and to provide a starting point for more elaborate applications of it, we have evaluated the spin-dependent structure functions $S^{\uparrow\uparrow}(k)=\frac{1}{2}[S(k)+S^{\sigma}(k)]$ and $S^{\uparrow\downarrow}=\frac{1}{2}[S(k)-S^{\sigma}(k)]$ associated with a Jastrow ground-state trial function (1) containing *state-independent* correlation factors of Schiff-Verlet type. That is, we take[39]

$$f(12)=f(r_{12})=\exp[-\tfrac{1}{2}(a/r_{12})^5]. \tag{50}$$

Such correlations have been studied recently in Refs. 5 and 9, with $a=2.888$ Å at $\rho=0.0142$ Å^{-3}.

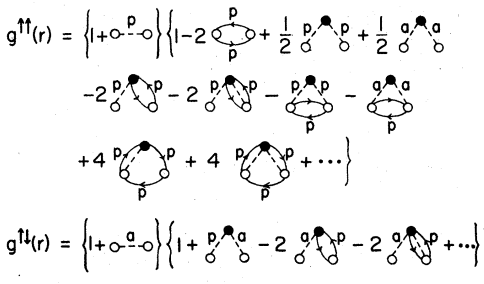

FIG. 14. Graphical representation of the cluster expansions of the radial distribution functions for pairs with parallel and opposite spin projections. As in Figs. 12–13, all diagrams are here to be interpreted simply as (multiple) integrals over $\vec{r}$ space.

In particular, Ref. 5 gives results for the spin-dependent structure functions derived via a Monte Carlo sampling algorithm, for 114 particles. It is of considerable interest to assess the degree of agreement of our Fermi hypernetted-chain evaluation with these Monte Carlo results.

The operator version of Eq. (44) is easily recast in momentum space, to yield a set of two algebraic equations for the quantities $S(k)$ and $S^{\sigma}(k)$ [or $S^{\uparrow\uparrow}(k)$ and $S^{\uparrow\downarrow}(k)$]. The operators G, P, ...are all of the type $\mathcal{O}(12)=\mathcal{O}(r_{12})+\mathcal{O}^{\sigma}(r_{12})\sigma_1\sigma_2$. Introducing the Fourier transforms $\mathcal{O}(k)=\rho\int \mathcal{O}(r)e^{i\vec{k}\cdot\vec{r}}d\vec{r}$ and $\mathcal{O}^{\sigma}(k)=\rho\int \mathcal{O}^{\sigma}(r)e^{i\vec{k}\cdot\vec{r}}d\vec{r}$, we obtain

$$[1+G(k)][1-P(k)]^2$$
$$=[1+\Delta L(k)]\{1+R(k)[1+\Delta L(k)]\} \tag{51}$$

together with a second equation which is of the same form but with functions $\mathcal{O}(k)$ replaced by $\mathcal{O}^{\sigma}(k)$. These equations determine, respectively, the structure function $S(k)\equiv 1+G(k)$ and the spin structure function $S^{\sigma}(k)\equiv 1+G^{\sigma}(k)$.

For state-independent correlations we have $R^{\sigma}(r)=P^{\sigma}(r)=0$. The equation for $S^{\sigma}(k)$ then collapses to

$$S^{\sigma}(k)=1+\Delta L^{\sigma}(k); \tag{52}$$

that for $S(k)$, with $1+\Delta L(k)=L(k)$, of course simply reproduces Eq. (42):

$$S(k)=\frac{L(k)[1+R(k)L(k)]}{[1-P(k)]^2}\ . \tag{53}$$

The function $S^{\sigma}(k)-1$ (or rather its Fourier inverse) is represented graphically by circular-exchange diagrams, i.e., diagrams of the "*cc*" class of Refs. 1 and 18. Figure 15 gives the leading contributions to the diagrammatic cluster expansion of $\Delta L^{\sigma}(r)$ in terms of the renormalized bond $R(r)$. The latter function is determined from the bare dynamical bond $\eta(r)=f^2(r)-1$ via the Fermi HNC equations (40) – (41). In Fig. 15, $R(r)$ is depicted by a heavy dashed line. Besides $\Delta L^{\sigma}(r)$, the function

$$\Delta L(r)=L(r)-\rho^{-1}\delta(r)=\Delta L^{\sigma}(r)+L_2(r) \tag{54}$$

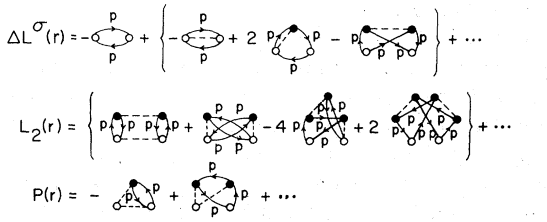

FIG. 15. Graphical representation of the leading terms of the expansions defining the functions $\Delta L^{\sigma}(r)$, $L_2(r)$, and $P(r)$. All diagrams are to be interpreted as integrals over $\vec{r}$ space and contain one or two renormalized bonds $R(r)$.

contains a sum of terms $L_2(r)$ represented by diagrams of the exchange-exchange or "*ee*" class of Refs. 1 and 18. The diagrams contributing to the renormalized-bond expansion of $L_2(r)$ must involve at least two heavy dashed lines; those with exactly two are shown in Fig. 5. This figure also displays the leading diagrammatic contributions to the function $P(r)$ entering formula (53).

The version of Fermi HNC (FHNC) theory adopted in the present work is especially suited to explication of the low-k behavior of the structure functions (34) and the relation of this behavior to the asymptotic properties of the correlation operator (6). For a state-independent correlation function with asymptotic behavior

$$f(r) \sim 1 + \lambda/4\pi^2 r^2, \quad r \to \infty, \tag{55}$$

the spin-averaged structure function is found to have the long-wavelength behavior[1,40]

$$S(k) \sim \alpha_F (1 - \lambda\rho\alpha_F)^{-1} k, \quad k \to 0^+. \tag{56}$$

Here, $\alpha_F = 3/4k_F$ is the slope, as $k \to 0^+$, of the structure function $S_F(k)$ of noninteracting fermions. For a "short-range" correlation function like (50), one has $\lambda = 0$ and the slope of $S(k)$ as $k \to 0^+$ coincides with that of the free Fermi gas.

It follows from Eq. (52) that the spin structure function $S^\sigma(k)$ associated with a state-independent correlation factor has the property

$$S^\sigma(k) \sim \alpha_F k, \quad k \to 0^+ . \tag{57}$$

(One need only note that the low-k behavior of $\Delta L^\sigma(k)$ is governed by the first term in its renormalized-bond cluster expansion, Fig. 15.) The result (57) holds for "long-range" spatial correlations [with asymptotic form (55)] as well as "short-range" correlations [e.g., choice (50)]. We can obtain a differing slope of $S^\sigma(k)$ at $k = 0^+$, meaning $S^\sigma(k) \sim \alpha k (k \to 0^+)$ with $\alpha \neq \alpha_F$, if spin-dependent correlations of long range are present in the trial

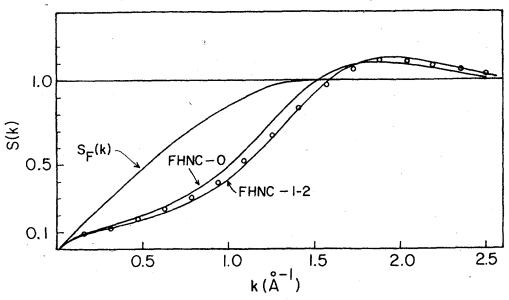

FIG. 16. Theoretical structure function $S(k)$ of liquid ^{3}He at density $\rho = 0.0142$ Å^{-3}, for Schiff-Verlet correlation functon (50), in the indicated FHNC– approximations. The circles are Fermi Monte Carlo results of Ceperley, Chester, and Kalos.[5] Also shown for comparison is the structure function $S_F(k)$ of the noninteracting Fermi gas.

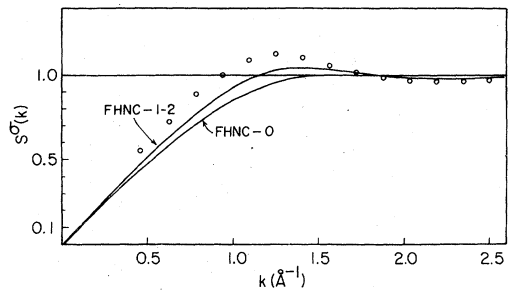

FIG. 17. Theoretical spin structure functions $S^\sigma(k)$ of liquid ^{3}He at density $\rho = 0.0142$ Å^{-3}, for Schiff-Verlet correlation function (50), in the indicated FHNC– approximations. The circles are Fermi Monte Carlo results of Ceperley, Chester, and Kalos.[5]

function (4), i.e., if we entertain a state-dependent correlation factor with asymptotic form

$$f(12) \sim 1 + (\lambda_m + \lambda_s \sigma_1 \sigma_2)/4\pi^2 r^2, \quad r \to \infty. \tag{58}$$

Thus, at least in principle, experimental determination of the spin structure function $S^\sigma(k)$ at low wave numbers may yield valuable information on the presence or absence of a λ_s component in the ground-state correlations of normal liquid ^{3}He.

Our numerical evaluation of the structure functions is based on choice (50), the structural Eqs. (52)–(54), and the Fermi HNC Eqs. (40)–(41). The hypernetted-chain procedure begins with the FHNC–0 approximation,[1] which is defined by setting $L(k) = S^\sigma(k) = S_F(k)$, $P(k) = B(k) = 0$. An improved approximation incorporates the contributions to $L(r)$ and $L^\sigma(r)$ containing one renormalized bond and the contributions to $P(r)$ with two such bonds. This approximation, deemed to be rather accurate,[41] is labeled FHNC–1-2. Referring to Fig. 15, it corresponds to truncating the $\Delta L^\sigma(r)$ and $P(r)$ expansions at the dots and dropping $L_2(r)$ altogether.

The results for $S(k)$, $S^\sigma(k)$, and $S^{\uparrow\downarrow}(k)$ are plotted in Figs. 16, 17 and 18, respectively. For comparison, we also include data points derived from Fourier transformation of the Fermi Monte Carlo

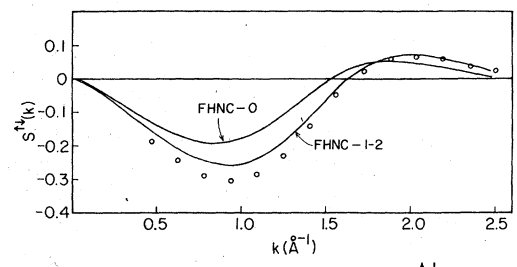

FIG. 18. Theoretical structure function $S^{\uparrow\downarrow}(k)$ for antiparallel spins in liquid ^{3}He at density $\rho = 0.0142$ Å^{-3}, for Schiff-Verlet correlation function (50), in the indicated FHNC– approximations. The circles are Fermi Monte Carlo results of Ceperley, Chester, and Kalos.[5]

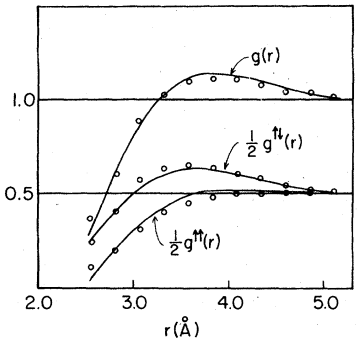

FIG. 19. Theoretical radial distribution functions of liquid ^{3}He at density $\rho = 0.0142$ Å^{-3}, for Schiff-Verlet correlation function (5), in the indicated FHNC− approximations. The circles are Fermi Monte Carlo results of Ceperley, Chester, and Kalos.[5]

results for spin-dependent radial distribution functions.[42]

It is seen from Figs. 16–18 that the behavior of the structure functions expressed by Eqs. (56) and (57) with $\lambda = 0$ is correctly reproduced by our numerical procedure. On the other hand, the Monte Carlo results at small k values ($k \leq 0.5$ Å^{-1}), which are shown in Fig. 2 of Ref. 5, violate properties (56) and (57) and are therefore incorrect. [To avoid confusion in the present comparison, we point out that $S_U(k)$ should be interchanged with $S_L(k)$ in the legend of Fig. 2b of Ref. 5.] The generally good agreement between the FHNC−1-2 results and the Monte Carlo results is very encouraging. Significant differences occur only for the functions $S^{\sigma}(k)$ and $S^{\uparrow\downarrow}(k)$, at k values in the range 0.5 Å$^{-1} \leq k \leq 1.2$ Å^{-1}. In seeking the origin of these differences it might be worthwhile to execute a further step in the FHNC− approximation scheme or to try the FHNC− scheme of Fantoni and Rosati.[1,11]

In some respects the agreement of FHNC− and Monte Carlo results appears more impressive if we transform the structure functions to coordinate space, forming the radial distribution functions $g(r)$, $g^{\sigma}(r)$, $g^{\uparrow\uparrow}(r)$, and $g^{\uparrow\downarrow}(r)$. Our numerical results are compared with Monte Carlo data[42] in Fig. 19. We should reiterate at this point that the FHNC− scheme is designed to generate reliable approximations to the *structure functions* of liquid ^{3}He for the chosen trial wave function. However, it is not to be expected that at the level of FHNC− approximation implemented here the Fourier inverses of $S(k) - 1$, etc. will yield reliable results for the above spatial distribution functions at small distances, $r \leq 2.2$ Å, where the repulsive portion of the interatomic potential dominates.[1] Thus, the FHNC− and Monte Carlo studies are complementary in the sense that the FHNC− procedure

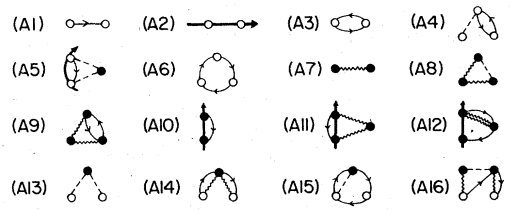

FIG. 20. Diagrams representing the analytic expressions of the appendix.

is good at small k where the Monte Carlo method is poor, while the latter is good at small r, where the former fails.

The numerical example just presented demonstrates the feasibility of performing accurate calculations of the spin-dependent structure functions $S^{\uparrow\downarrow}(k)$ and $S^{\uparrow\uparrow}(k)$ using the methods of Sec. IV, these functions being key inputs to a determination of the one-body density matrix and related quantities as described in Secs. II, III, and IV. Our program is currently being applied to the treatment of correlations (6) in full generality.

With the incorporation of spin-density fluctuations via (6), we expect a significant improvement in the description of the structure functions $S^{\sigma}(k)$ and $S^{\uparrow\downarrow}(k)$ and, further, of the magnetic susceptibility of liquid ^{3}He. On the other hand, the spin-averaged structure function $S(k)$ and (consequently) the energy per particle are presumably not much affected by the presence of $\zeta^s(r_{12})$ of Eq. (11). Explicit consideration of spin-density fluctuations is thought to be of vital importance to the development of a successful correlated pairing theory of superfluid ^{3}He.[43] The methods we have expounded may be instrumental to the achievement of this goal.

APPENDIX: GENERALIZED GRAPHICAL REPRESENTATION OF FERMI CLUSTERS

It is instructive to apply the generalized diagrammatic rules of Sec. II to a selection of typical cluster expressions. In Fig. 20 we supply the diagrammatic representations of the following components:

$$l(12) = \tfrac{1}{2}(1 + \sigma_1\sigma_2)l(k_F r_{12}), \tag{A1}$$

$$A^{-1}e^{i\vec{k}\cdot\vec{r}_{12}}, \tag{A2}$$

$$l^2(12), \tag{A3}$$

$$\eta(13)l^2(23), \tag{A4}$$

$$A^{-1}e^{i\vec{k}\cdot\vec{r}_{12}}l(12)\eta(13)\eta(23), \tag{A5}$$

$$l(12)l(13)l(23), \tag{A6}$$

$$\sum_{ij}\langle ij\,|\,\xi(12)\,|\,ij\rangle=\frac{1}{4}\rho^2\sum_{s_1s_2}\int d\vec{r}_1\,d\vec{r}_2\langle s_1s_2\,|\,\xi(12)\,|\,s_1s_2\rangle, \tag{A7}$$

$$\sum_{ijk}\langle ijk\,|\,\xi(12)\xi(13)\eta(23)\,|\,ijk\rangle=\frac{1}{8}\rho^3\sum_{s_1s_2s_3}\int d\vec{r}_1\,d\vec{r}_2\,d\vec{r}_3\langle s_1s_2s_3\,|\,\xi(12)\xi(13)\eta(23)\,|\,s_1s_2s_3\rangle, \tag{A8}$$

$$\sum_{ijk}\langle ijk\,|\,\xi(12)\xi(13)\,|\,ijk\rangle=\frac{1}{8}\rho^3\sum_{s_1s_2s_3}\int d\vec{r}_1\,d\vec{r}_2\,d\vec{r}_3\langle s_1s_2s_3\,|\,\xi(12)\xi(13)l^2(23)\,|\,s_1s_2s_3\rangle, \tag{A9}$$

$$\sum_{i}\langle i\hat{k}\,|\,\hat{k}i\rangle=\Theta(k_F-k)=\frac{1}{4}\rho^2\sum_{s_1s_2}\frac{1}{A}\int d\vec{r}_1\,d\vec{r}_2\langle s_1s_2\,|\,e^{i\vec{k}\cdot\vec{r}_{12}}l(12)\,|\,s_1s_2\rangle, \tag{A10}$$

$$\sum_{ij}\langle i\hat{k}j\,|\,\xi(13)\xi(23)\,|\,\hat{k}ij\rangle=\frac{1}{8}\rho^3\sum_{s_1s_2s_3}\frac{1}{A}\int d\vec{r}_1\,d\vec{r}_2\,d\vec{r}_3\langle s_1s_2s_3\,|\,e^{i\vec{k}\cdot\vec{r}_{12}}l(12)\xi(13)\xi(23)\,|\,s_1s_2s_3\rangle, \tag{A11}$$

$$\sum_{ij}\langle\hat{k}ij\,|\,\xi^2(23)\,|\,j\hat{k}i\rangle=\frac{1}{8}\rho^3\sum_{s_1s_2s_3}\frac{1}{A}\int d\vec{r}_1\,d\vec{r}_2\,d\vec{r}_3\langle s_1s_2s_3\,|\,e^{i\vec{k}\cdot\vec{r}_{12}}\xi^2(23)l(23)l(13)\,|\,s_1s_2s_3\rangle, \tag{A12}$$

$$\frac{1}{2}\rho\sum_{s_3}\int d\vec{r}_3\langle s_3\,|\,\eta(13)\eta(23)\,|\,s_3\rangle, \tag{A13}$$

$$\frac{1}{2}\rho\sum_{s_3}\int d\vec{r}_3\langle s_3\,|\,\xi(13)\xi(23)l(13)l(23)\,|\,s_3\rangle, \tag{A14}$$

$$\frac{1}{2}\rho\sum_{s_3}\int d\vec{r}_3\langle s_3\,|\,\eta(13)l(13)l(12)l(23)\,|\,s_3\rangle, \tag{A15}$$

$$\frac{1}{4}\rho^2\sum_{s_3s_4}\int d\vec{r}_3\,d\vec{r}_4\langle s_3s_4\,|\,\xi(13)\xi(24)\eta(34)l(14)l(24)\,|\,s_3s_4\rangle. \tag{A16}$$

ACKNOWLEDGMENTS

Part of this work was done while M. L. Ristig was enjoying the hospitality of the Niels Bohr Institute, Copenhagen. Thanks are due to D. Ceperly for providing Monte Carlo data on the spin-dependent structure functions and radial distribution functions. We gratefully acknowledge financial support by the Minister für Wissenschaft und Forschung des Landes Nordrhein-Westfalen under Grant No. 06/0604/68511 and by the NSF under Grant Nos. DMR 76-14929 and DMR 77-12263.

[1] J. W. Clark, Prog. Part. Nucl. Phys. (to be published).
[2] B. D. Day, Rev. Mod. Phys. 50, 495 (1978).
[3] J. G. Zabolitzky, Phys. Rev. A 16, 1258 (1977).
[4] E. Krotscheck, J. Low Temp. Phys. 27, 199 (1977).
[5] D. Ceperley, G. V. Chester, and M. H. Kalos, Phys. Rev. B 16, 3081 (1977).
[6] M. L. Ristig and J. W. Clark, Phys. Rev. B 14, 2875 (1976).
[7] P. M. Lam, H. W. Jackson, M. L. Ristig, and J. W. Clark, Phys. Lett. A 58, 454 (1976).
[8] P. M. Lam, J. W. Clark, and M. L. Ristig, Phys. Rev. B 16, 222 (1977).
[9] J. W. Clark, P. M. Lam, J. G. Zabolitzky, and M. L. Ristig, Phys. Rev. B 17, 1147 (1978).
[10] E. Krotscheck and M. L. Ristig, Phys. Lett. A 48, 17 (1974); Nucl. Phys. A 242, 389 (1975).
[11] S. Fantoni and S. Rosati, Nuovo Cimento Lett. 10, 545 (1974); Nuovo Cimento A 25, 593 (1975).
[12] E. Krotscheck, Phys. Lett. A 54, 123 (1975).
[13] E. Feenberg, *Theory of Quantum Fluids* (Academic, New York, 1969).
[14] J. M. J. van Leeuwen, J. Groeneveld, and J. de Boer, Physica 25, 792 (1959).
[15] J. W. Clark, P. M. Lam, and W. J. Ter Louw, Nucl. Phys. A 255, 1 (1975).
[16] K. E. Kürten, M. L. Ristig, and J. W. Clark, Phys. Lett. B 74, 153 (1978); Nucl. Phys. A (to be published).
[17] V. R. Pandharipande and R. B. Wiringa, Nucl. Phys. A 266, 269 (1976).
[18] R. B. Wiringa and V. R. Pandharipande, Nucl. Phys. A 299, 1 (1978).
[19] S. Fantoni and S. Rosati, Nuovo Cimento A 43, 413 (1978).
[20] O. Benhar, C. Ciofi degli Atti, S. Fantoni and S. Rosati, Phys. Lett. B 70, 1 (1977).
[21] M. L. Ristig, W. J. Ter Louw, and J. W. Clark, Phys. Rev. C 3, 1504 (1971); 5, 695 (1972).
[22] K. E. Kürten and M. L. Ristig, Phys. Lett. B 66, 113

(1977).
[23]D. Pines, *Elementary Excitations in Solids* (Benjamin, New York, 1963).
[24]P. M. Platzman and P. Eisenberger, Solid State Comm. 14, 1 (1974).
[25]R. Scherm, W. G. Stirling, A. D. B. Woods, R. A. Cowley, and G. J. Coombs, J. Phys. C 7, L341 (1974).
[26]K. Sköld, C. A. Pelizzari, R. Kleb, and G. E. Ostrowski, Phys. Rev. Lett. 37, 842 (1976).
[27]V. F. Sears, J. Phys. C 9, 409 (1976).
[28]Y. Narahara, J. Phys. Soc. Jpn. 24, 169 (1967).
[29]E. K. Achter and L. Meyer, Phys. Rev. 188, 291 (1969).
[30]R. B. Hallock, Phys. Rev. Lett. 26, 618 (1971); J. Low Temp. Phys. 9, 109 (1972).
[31]F. A. Stevens, Jr., and M. A. Pokrant, Phys. Rev. A 8, 990 (1973).
[32]S. Fantoni, Nuovo Cimento A 44, 191 (1978).
[33]L. J. Lantto and P. J. Siemens, Phys. Lett. B 68, 308 (1977).
[34]C. E. Campbell and E. Feenberg, Phys. Rev. 188, 396 (1969).
[35]E. Krotscheck, Nucl. Phys. A 293, 293 (1977).
[36]E. Krotscheck (private communication).
[37]E. Meeron, J. Math. Phys. 1, 192 (1960).
[38]R. A. Smith, Invited Talk at the Urbana Workshop on Nuclear and Dense Matter, May, 1977 (unpublished).
[39]D. Schiff and L. Verlet, Phys. Rev. 160, 208 (1967).
[40]E. Krotscheck, Nuovo Cimento Lett. 14, 219 (1975).
[41]E. Krotscheck, Nucl. Phys. A 293, 293 (1977); Nucl. Phys. A (to be published).
[42]D. Ceperley (private communication).
[43]T. C. Paulick and C. E. Campbell, Phys. Rev. B 16, 2000 (1977).